

Thesis - 1952 - Carothers

UNIVERSITY OF CALIFORNIA - BERKELEY

UCRL-

**UNCLASSIFIED**

CERN LIBRARIES, GENEVA

CERN LIBRARIES, GENEVA



P00037416

**RADIATION LABORATORY**

# 2205926

UCRL-1829  
Unclassified-Physics Distribution

UNIVERSITY OF CALIFORNIA

Radiation Laboratory

Contract No. W-7405-eng-48

ON THE RATIO OF  $\pi^+$  TO  $\pi^-$  MESONS PRODUCED BY GAMMA RAYS

James Edward Carothers

(Thesis)

June, 1952

Berkeley, California

## TABLE OF CONTENTS

### I Introduction

### II Experimental Procedure

#### A. The Detection Scheme

#### B. The Detection Apparatus

- 1) Arrangement of the Apparatus
- 2) The Counters
- 3) The Coincidence Circuit and Associated Electronics
- 4) The Magnet
- 5) Resolution in Energy and Angle

### III Results

#### A. Corrections to the Data

#### B. Procedure

#### C. Values Obtained

### IV Acknowledgments

### V References

ON THE RATIO OF  $\pi^+$  TO  $\pi^-$  MESONS PRODUCED BY GAMMA RAYS

James Edward Carothers

ABSTRACT

The minus to plus production ratio for pi mesons produced in the 320 Mev photon beam of the Berkeley synchrotron has been measured at  $60^\circ$ ,  $90^\circ$ , and  $150^\circ$  to the beam for beryllium and at  $90^\circ$  for carbon. Identification of the mesons was made by using a magnet to select a desired momentum interval, and measuring the velocity of the particles delivered by the magnet. The results were

	Be	C
$60^\circ$	$1.93 \pm 0.12$	
$90^\circ$	$1.96 \pm 0.10$	$1.27 \pm 0.06$
$150^\circ$	$1.92 \pm 0.11$	

The relative production of positive and negative mesons at  $90^\circ$ , per proton for positives and per neutron for negatives, from beryllium and carbon was:

$$\frac{\pi^+ \text{Be}}{\pi^+ \text{C}} = 1.24 \pm 0.09 \quad \frac{\pi^- \text{Be}}{\pi^- \text{C}} = 1.44 \pm 0.08$$

The limits shown are in terms of standard deviation.

ON THE RATIO OF  $\pi^+$  TO  $\pi^-$  MESONS PRODUCED BY GAMMA RAYS

James Edward Carothers

I INTRODUCTION

The first experiments on the production of charged mesons by photons<sup>1,2</sup> indicated that the negative to positive ratio was greater than one for mesons produced from a carbon target. Calculations made by Brueckner and Goldberger<sup>3</sup>, and by Brueckner<sup>4</sup> for free nucleons show that this result can be predicted whether the interaction of the electromagnetic field of the photon is with the currents produced by the moving charged particles (proton and mesons) or with the magnetic moment of the interacting nucleon. The two interactions lead, however, to a different dependence of the ratio on emission angle and energy.

If the electric dipole interactions predominate, the expression obtained by Brueckner for the ratio is

$$\frac{\sigma_+}{\sigma_-} = \left[ 1 - \frac{q_0}{Mc^2} (1 - v/c \cos \theta) \right]^2 \quad (1)$$

where  $q_0$  is the total meson energy  
 $M$  is the nucleon mass  
 $v$  is the meson velocity  
 $\theta$  is the angle between the meson and nucleon velocity  
vectors.

The solid curves in Fig. 1 show the dependence on meson energy and emission angle of this expression. The ratio rises rapidly at large angles, and the variation with energy at large angles is also rapid.

If, on the other hand, the interaction is primarily between the electromagnetic field and the magnetic moment of the nucleons, the expression for the ratio is

$$\frac{\sigma_+}{\sigma_-} = \left[ 1 - \frac{\gamma_p - \gamma_n}{\gamma_p + \gamma_n} \frac{q_0}{Mc^2} (1 - v/c \cos \theta) \right]^2 \quad (2)$$

where  $\gamma_n$  and  $\gamma_p$  are the magnitudes of the magnetic moments of the neutron and proton and other symbols have the same meaning as in (1).

This expression is the same as that for the electric dipole interaction, except that the effect of the term giving the energy and angle dependence is lessened by the ratio

$$\frac{\gamma_p - \gamma_n}{\gamma_p + \gamma_n} \quad (3)$$

If the values of the nucleon moments observed in a static field are put into this expression, the ratio is given by

$$\frac{\sigma_+}{\sigma_-} = \left[ 1 - \frac{0.2 q_0}{Mc^2} (1 - v/c \cos \theta) \right]^2 \quad (3)$$

The values of this expression are given by the dotted curves in Fig. 1. A ratio close to unity, with very little dependence on energy and angle, is shown.

Measurements of the minus to plus ratios have been made for several elements by various experimenters. The values thus far obtained are summarized in Table 1. The only measurement of the angular variation of the ratio over at least  $90^\circ$  is that of Peterson, Gilbert, and White<sup>2</sup> for carbon at  $45^\circ$ ,  $90^\circ$ , and  $135^\circ$ . No variation with angle was observed, to within the statistics obtained in the experiment. While the data indicated that a magnetic interaction was to be expected, no

TABLE 1

Element	Angle	Ratio	Detection	Reference
D	45°	0.96 ± 0.11	Plates	5
D	90°	0.98 ± 0.14	Plates	5
D	26°	0.90 ± 0.23	Plates	10
D	90°	0.5 ± 0.5	Plates	10
D	135°	1.19 ± 0.12	Double magnet	8
He	45°	0.99 ± 0.15	Plates	13
Be	90°	2.2 ± 0.2	Plates	11
Be	135°	2.40 ± 0.2	Double magnet	12
Be	135°	2.25 ± 0.11	Double magnet	8
C	45°	1.29 ± 0.22	Plates	2
C	90°	1.30 ± 0.12	Plates	2
C	135°	1.34 ± 0.20	Plates	2
C	135°	1.12 ± 0.07	Double magnet	12
C	135°	1.04 ± 0.05	Double magnet	8
C	26°	1.03 ± 0.25	Plates	10
C	90°	1.43 ± 0.13	Plates	10
O	135°	1.02 ± 0.1	Double magnet	8
F	135°	1.41 ± 0.1	Double magnet	8
Al	135°	1.20 ± 0.1	Double magnet	8
S	135°	0.82 ± 0.08	Double magnet	8
Ca	135°	0.58 ± 0.06	Double magnet	8
Bi	135°	1.32 ± 0.12	Double magnet	8

conclusions regarding the values of the magnetic moments to be used in equation two could be made.

A better measurement of the angular variation of the ratio would decide more definitely between a predominately electric and predominately magnetic interaction. If, as seemed indicated by the work of Peterson, Gilbert, and White, the interaction were primarily magnetic in nature, it would also be possible to check the validity of using the values of the static nucleon moments in equation two. This, however, would require the assumption that the angular variation of the ratio from a complex nucleus is the same as that from free nucleons. It would further require statistics that could detect a ten to twenty per cent change in the ratio.

The electronic detection scheme described in the following paper seemed to offer a means of obtaining sufficient data with a good degree of freedom from systematic errors in the determination of the ratio. Measurement of the ratio was therefore undertaken at angles of  $150^\circ$ , the largest angle that could be physically achieved,  $90^\circ$ , and  $60^\circ$ , which was the farthest forward that background conditions permitted measurements.

## II EXPERIMENTAL PROCEDURE

### The Detection Scheme

It is desirable that the measurement of the minus to plus ratio be carried out in a manner that satisfies the following criteria:

- 1) The positive and negative meson production should be measured at the same time with identical apparatus. This assures that identical beam conditions are obtained for both types of production, and eliminates difficulties connected with monitoring the primary beam.

It is, of course, virtually impossible to construct sets of counting apparatus, channeling, etc. that have identical efficiencies. However, it is possible to use two counting channels in such a way that the detection efficiencies do not affect the value of the ratio obtained. If a magnet is used to separate the mesons of one charge, and to deliver them to the two detectors, when the magnetic field is reversed only the sign of the mesons in the detectors is changed. If the efficiencies of the detectors are the same for both positive and negative mesons, they cancel in a measurement of the ratio.

2) The detection and identification of the mesons should be independent of the special properties of the positive and negative pi mesons, i.e. the  $\pi^+ \rightarrow \mu^+ \rightarrow \beta^+$  decay scheme and the star formation by the  $\eta^-$ . This allows the efficiencies of the detectors to be the same for the two particles.

At the time this experiment was undertaken, no electronic counting apparatus satisfying this condition existed. An electronic method for positive pi detection had been developed by Steinberger and Bishop<sup>6</sup> using a delayed coincidence between the  $\pi^+$  and  $\beta^+$  in the  $\pi^+ \rightarrow \mu^+ \rightarrow \beta^+$  decay as the identification. This method was extended by Jakobson, Schulz, and Steinberger<sup>7</sup> to include the  $\pi^+ \rightarrow \mu^+$  decay. No possibility of counting negative pi mesons by such a method exists however, since the ones that are brought to rest in matter are absorbed in a time much shorter than the decay time.

Littauer and Walker<sup>8</sup> have developed an apparatus using double focusing magnets which is capable of selecting mesons emitted at  $135^\circ$  and eliminating almost all electron background. They have measured the ratios for several elements, but their work, to the present time, has been at a single angle.

Photographic emulsions offered the first means of measuring both positive and negative mesons and several ratios have been obtained in this way by the authors cited in Table 1. This method does not satisfy the second condition above in that it requires the observer to detect and identify different types of track endings with the same efficiency.

The quantities common to both the positive and negative pi mesons, which are most susceptible to measurement, are the momentum, the total kinetic energy, the rate of energy loss per unit distance in an absorber, the velocity, and the total range. Measurement of two of these quantities is sufficient to identify the particle being considered (with the exception of the combination of the velocity and the rate of energy loss, since both depend only on the velocity).

A magnetic field is necessary to achieve charge separation of the mesons. This gives one identification parameter also, since the channel that separates the positive and negative mesons can also select a desired momentum interval. The charged particle background at the synchrotron is, of course, almost entirely positive and negative electrons, with energies up to 300 Mev. This means that the magnetic channel will pass some electrons, since  $H\rho$  values for 20 to 100 Mev mesons are the same as for 75 to 195 Mev electrons. The second identification parameter should thus be chosen to distinguish best between these high energy electrons and the mesons.

For electrons with energies of many Mev, the range, energy loss per unit distance, and the total energy lost in a given absorber thickness are quantities which can be quite different for two electrons with the same momentum due to the different ways in which they can shower and scatter in the absorber.

In contrast to these quantities, the velocity of an electron of a few Mev or over varies over a very small range, e.g. from a  $\beta$  of 0.96 for a 5 Mev electron to a  $\beta$  of 0.99<sup>+</sup> for a 320 Mev electron. Consequently, if a velocity determination is made, all of the primary background will occur very close to  $\beta$  of 1.0. Since the meson production for a 320 Mev photon beam is largely below 100 Mev, the  $\beta$  of the mesons will fall between 0 and 0.8. In particular, 40 to 50 Mev pi mesons have a  $\beta$  between 0.63 and 0.68. Thus, if we work with 45 Mev mesons, the requirement on a velocity selector is that it have good discrimination between a  $\beta$  of 1 and a  $\beta$  of 0.66.

The primary objection to the use of a velocity measurement as a means of particle identification is that it requires timing the flight of the particle over a distance which is relatively large compared to normal target-counter distances. This makes the solid angle intercepted by the counters quite small. The distance used depends on the time resolution possible and the accuracy necessary in the time measurement, and it is obviously desirable to use the fastest resolution circuit available in order to minimize the loss in solid angle.

The crystal diode bridge circuit developed by Mr. Leland Neher of this laboratory is capable of a time resolution of about  $10^{-9}$  seconds with good counting efficiency. It seemed that it would be possible to use this circuit as a suitable velocity selector, since the time difference between a high energy electron and a 45 Mev meson traveling over 150 centimeters is  $2.5 \times 10^{-9}$  seconds. Calculations using cross sections as determined by Peterson, Gilbert, and White<sup>2</sup> indicated that a counting rate of about 60 to 120 mesons per hour might be expected at normal synchrotron operating intensities. This is a feasible rate

if the background is low, and it seemed reasonable to expect a very low background using good velocity discrimination.

The Detection Apparatus

Arrangement of the Apparatus Before a detailed description of the apparatus is given, the physical arrangement will be described. Figure 2 shows a schematic diagram of the apparatus at  $90^{\circ}$  to the beam, together with the electronic components that are located in the magnet room during a run.

Two magnetic channels are used with each utilizing three stilbene-photomultiplier counters to make two double coincidences. The first coincidence circuit has a resolution of about  $10^{-9}$  seconds and is used as the velocity selector. The second circuit has a resolution of about  $5 \times 10^{-9}$  seconds and is mixed with the first (see Fig. 7) in a slow mixer to reduce the statistical accidentals.

The small magnet shown had pole faces 4 in. by 13 in. and was capable of about six kilogauss over a two inch gap. This arrangement allowed a  $30^{\circ}$  deflection which was sufficient to eliminate any straight line paths between the front and rear counters.

Shielding was used primarily to reduce the singles counting rates due to particles coming from the synchrotron itself and from the beam collimator. The front counters could not be shielded from the target and the rear counters received very few particles from the target, since they were nearly eight feet away.

The Counters In order to make a coincidence circuit with a resolving time of the order of  $10^{-9}$  seconds, pulses of this duration must be available. It is further desirable that the amplitude of all pulses be the same.

Measurements by Post and Shiren<sup>9</sup> have shown that the pulses from a 1P21 photomultiplier tube viewing a stilbene crystal phosphor have a decay time of  $6.6 \times 10^{-9}$  seconds, with a rise time of about a tenth of this. Such pulses, fed to the limiter whose circuit diagram is given in Fig. 3 and then clipped by a 10 centimeter shorted line (RG 8U), give pulses that have the desired uniform amplitude and short duration.

The counters used in the time of flight telescope were all stilbene crystals viewed by 1P21 photomultiplier tubes. The front phosphor was a stilbene crystal 2 1/2 inches square by 1/4 inch thick. Since a crystal this thin is very fragile, it was enclosed in a lucite box with 1/16 inch windows and 1/4 inch walls. The space between the crystal and the lucite was filled with mineral oil to minimize reflections at the interfaces. This phosphor was viewed by two phototubes situated on opposite sides of the crystal, in order that the two channels should see the same particles entering the magnet. Such an arrangement proved to be necessary when it was found that the signal from one tube, when split and used for both channels, was too small in amplitude to trigger the bridge circuits.

Since the rear counters are at about 200 centimeters from the target, a large counting area is needed to obtain sufficient solid angle to make the experiment feasible. The size of a single counter is limited to about 5 x 8 centimeters, however, due to the time required for the light from the scintillation to travel from the point of origin to the photocathode. Figure 4 illustrates this effect. The time difference between paths 1 and 2 or 3 and 2 is very small, compared to  $10^{-9}$  seconds. However, the time required for the light to travel from A to the photocathode K adds directly to the time required to travel path 1. In stilbene,

which has an index of refraction of about 1.5, the time required to travel this extra 7 centimeters (in a 5 x 8 centimeter crystal) is  $3.5 \times 10^{-10}$  seconds. A similar situation obtains for path 3, with the difference that here the extra time appears in the front counter signal. There is therefore, a time uncertainty of  $\pm 3$  to  $4 \times 10^{-10}$  seconds introduced by the crystals which were used. This uncertainty increases with crystal size, and would necessitate a further increase in counter separation to obtain the same relative discrimination between different velocities were the phosphors to be made larger than 5 x 8 centimeters. It was this inherent limitation which prevented the use of considerably larger counters.

The alternative to large single counters is the use of many small crystals, each with its own phototube and limiter, with all the signals going to a single bridge junction. Four crystals with associated phototubes and limiters can be used successfully in this way, but the use of more tubes than this presents considerable difficulty. It is difficult to place more than four tubes together in such a way that the crystals effectively cover the desired area. The reflection of the signals at the junction where the cables come together acts to diminish the amplitude of the signals to the bridge and also to increase the effective singles rates seen by the bridge circuit. In most of the runs two crystals were used and no difficulty was encountered from the signal mixing.

Associated with each photomultiplier was the pulse amplitude limiter. This was constructed as close to the phototube as was physically possible in order to reduce the loss of high frequency signal components due to the stray capacity present in long leads. Operation of the photomultiplier at voltages of from 1500 to 1700 volts was necessary to obtain

pulses large enough to provide efficient limiting action.

These limiters were capable of about a one megacycle repetition rate, and it was this limitation which prescribed the allowable singles rates in the counters. The electron background in the front counter rises very rapidly at the forward angles, and it was not possible to observe at angles smaller than  $60^\circ$  if no more than 10 percent dead time due to target background was allowed. A decrease in beam intensity to decrease the singles rate would not have been practical due to the low counting rate obtained even at full beam.

The stilbene crystals used in the experiment were grown by Mr. Calvin André and the author.

The Coincidence Circuit and Associated Electronics A diagram of the bridge circuit and pre-amplifier developed by Mr. Leland Neher is shown in Fig. 5. The response of the circuit to electrons coming from a target in the synchrotron beam is shown in Fig. 6. As previously discussed, these electrons all have essentially the same velocity.

The characteristics of the resolution curve that are important for the experiment are the change in counting rate as a function of time difference from the coincidence time and the degree of symmetry about the coincidence time. The response, in terms of percent of peak counting rate at a given time difference, has been found to be quite reproducible from run to run, with values as given in Fig. 6. At  $1 \times 10^{-9}$  seconds delay the counting rate is about 50 percent; at  $2 \times 10^{-9}$  seconds, about 10 percent; and at  $3 \times 10^{-9}$  seconds about 3 percent. As would be expected for any circuit which involves the overlap of two similar pulses, the response is symmetric about the peak, and it is this which enables

us to measure the electron background to be found at the meson counting time delay. This is discussed in Section III.

The outputs of the fast and slow coincidence bridge units were sent through standard UCRL linear amplifiers and then into gate making units which produced one microsecond gates. These were mixed in a slow coincidence unit and the output, giving triple coincidences, was scaled. As shown on the block diagram of the electronics (Fig. 7), the output of the fast coincidence bridge was sent from the linear amplifier to three gate making units. The discriminators of these three units were set at three levels (e.g. 15, 25, 35 volts) and each output was mixed separately with the pulses from the slow coincidence bridge. These three gates were operated in this manner since it is quite difficult to obtain sufficient numbers to determine voltage and bias plateaus when mesons are being counted. Running three discriminators in parallel gave a check on the plateau characteristics for mesons while data was being taken, and at the same time a check on the consistency of the gate making-slow mixer combinations was available.

Each of the gate making units had output to a scaler as well as to the final mixer, and this gave a check on the operation of the bridge, linear amplifier, and gate combinations. The double coincidences in the  $10^{-9}$  second channel were about twice the triples rate. The  $5 \times 10^{-9}$  second channel doubles rate was two to three times the triples rate.

Due to the large amount of electrical background from the operation of the synchrotron, the scalers were gated off except for a time of about 5000 microseconds during which the beam pulse occurred.

Magnet The choice of a magnet for the experiment was influenced by the fact that the operation of the synchrotron is affected by very

small stray magnetic fields. Injection of the electrons occurs when the magnetic field in the orbit is about eight gauss, and stray fields of the order of one gauss can disturb the injection efficiency to such an extent that no beam can be obtained. For this reason, a small magnet with low leakage was constructed from parts previously used in bevatron model tests. This magnet had four by thirteen inch pole faces and gave fields of the order of six kilogauss over a two inch gap. With this magnet in position for a run, no effect on the synchrotron operation could be detected with the full field in either direction.

A magnet with a low leakage field also simplifies the shielding of the photomultiplier tubes. The front counter was located only six inches from the edge of the gap, but a one-eighth inch thick piece of soft iron sheet, with a two by three inch hole to permit passage of the particles, reduced the field at the photomultiplier position to less than two gauss.

The rear counters were positioned by using a current carrying wire to give the meson trajectories. Checks with the wire showed that reversing the magnetic field delivered particles of the opposite sign and the same momentum to the same position on the rear counters.

Resolution in Energy and Angle The momentum interval selected by the magnet and the velocity interval selected by the time of flight apparatus both act to determine the energy range of the particles accepted. However, the separation of counters used in this experiment gives a very poor energy resolution of particles with a  $\beta$  over 0.6. The momentum of particles delivered to the rear counters by the magnet covers a meson energy range of 36 to 54 Mev. These energies correspond to  $\beta$ 's between 0.61 and 0.69, and this gives a source of particles with

a time spread of about  $10^{-9}$  seconds in the time required to traverse the distance separating the counters. This time spread lies within the resolution of which the bridge circuit is capable, and there is thus little velocity selection possible for the mesons. Conversely, almost all of the mesons delivered by the magnet are counted by the velocity selector.

The target thickness gives a maximum energy loss sufficient to reduce 70 Mev mesons to 54 Mev, so the total energy range is from 36 to 70 Mev.

The large separation of the rear counters from the target makes the angular resolution of the counting system itself quite good. The ten centimeter spread of counters in the rear have an angular acceptance of about three degrees. The uncertainty in angle due to scattering within the target is larger than this and largely determines the spread in angle that is seen.

An estimate of the scattering within the target can be made using the usual multiple scattering formulas. For 55 Mev mesons, the mean scattering angle in the carbon target is about five degrees, and in the beryllium target about two degrees. Combined with the angular acceptance of the rear counters, the target scattering gives an angular spread of about plus or minus eight degrees for the carbon target and plus or minus four degrees for the beryllium.

### III RESULTS

#### Corrections to the Data

Spurious Counts Events which would be confused with a meson passing through the apparatus can originate from accidental coincidences due to the high singles rates in the counters, from electrons counted

because of the finite velocity resolution of the time of flight apparatus, and from electrons which scatter sufficiently to take the same time between counters as does a meson. A good measurement of the number of counts due to the first two causes can be obtained in one measurement by using the symmetry of the resolution curve. The experimentally obtained resolution curve shown in Fig. 6 shows that with a delay of  $2.5 \times 10^{-9}$  seconds from the true coincidence time, some counts are still obtained. Or, in terms of the particular experiment considered here, at a delay of 150 centimeters of RG 8U cable, corresponding to a  $\beta$  of 0.66, some counts due to electrons which should require only 100 centimeters of cable ( $\beta = 1.0$ ) appear on the scalers. However, the same number of counts due to the electrons occur at a delay of 50 centimeters, which is the position symmetric to 150 centimeters on the resolution curve. Accidental counts will be the same for any delay, and so a measurement at 50 centimeters gives a good value for both the accidental counts and the electron counts due to the finite velocity resolution of the apparatus. The background found in this way was less than 1 percent at  $150^\circ$ , about 5 percent at  $90^\circ$ , and about 10 percent at  $60^\circ$ .

No such direct method exists for measuring the number of electrons which scatter enough to take the same time as a meson. However, the extra path difference required would be 75 centimeters, and from the geometry of the counters and magnet, it does not seem possible for this to occur for any single scattering event. Multiple scatters should be rare enough to make this type of background very small.

Nuclear Absorption The targets used had a total thickness of 8.0  $\text{gm/cm}^2$  (Be) and 7.1  $\text{gm/cm}^2$  (C) in the direction of observation and if the nuclear absorption were different for positive and negative mesons,

the observed ratio would be different from the true ratio. Recent measurements<sup>14,15</sup> indicate that for the light elements the absorption cross sections for plus and minus pi mesons are in the ratio of about 0.7 to 1.0 with an absolute value close to the geometrical area. Using values of 265 millibarns for beryllium and 320 millibarns for carbon as the pi minus absorption cross sections, and 0.7 times these values for the pi plus cross sections, the corrections to the observed ratios would be 1 percent for beryllium and 2 percent for carbon. These corrections are not included in the values given in Table 2 or plotted in Fig. 8.

Procedure Six synchrotron runs were made to collect the data used to obtain the ratios given in Table 2. Five of these were two day runs, with two runs at 60°, two at 150°, and one at 90°, with a beryllium target in each case. The remainder of the beryllium data at 90°, and all of the carbon data was taken during one five day run, using the beam after it had passed through a high pressure gas target of another experimenter. This target placed a maximum of  $1.7/\text{cm}^2$  grams per square centimeter of stainless steel and  $5.2 \text{ grams}/\text{cm}^2$  of deuterium in the beam. The attenuation produced by this target was unnoticeable in the meson counting rates.

Large targets were used in order to utilize as much of the synchrotron beam as possible. The beryllium and carbon blocks used were  $4.4 \times 7.6 \times 10.2$  centimeters and were oriented so the large face was parallel to the front counter at each angle. This kept the energy loss of the mesons the same at each angle, but placed varying amounts of the target in the beam. The variation in amount of target is immaterial in the determination of the ratio. The change in target thickness in the beam direction was from 0.07 to 0.04 shower lengths, so no correction was made for change in beam composition due to target orientation.

Even with these large targets, the counting rate per channel was only about one half count per nunan. The synchrotron at this time was delivering a maximum beam of one nunan per minute, with an average over a day of about a half this. The counting rate per channel was thus between fifteen and thirty counts per hour.

During the course of a run, the magnetic field was reversed at intervals of about an hour. Background runs were made by periodically changing the delay cable length from 150 centimeters to 50 centimeters, as discussed in the previous section.

The data for carbon at  $90^\circ$  were obtained immediately after a beryllium run. No changes in the apparatus other than a change of target were made. Since the portion of the target seen by the magnet channels was not known exactly, the carbon and beryllium targets were made to have the same physical dimensions. This gives a different effective amount of target in the two cases, due to the different densities of the carbon and the beryllium, but the effective extent is unchanged.

Values Obtained The minus to plus ratio was measured at  $60^\circ$ ,  $90^\circ$ , and  $150^\circ$  to the beam for beryllium, and at  $90^\circ$  for carbon. The values obtained, uncorrected for nuclear absorption in the target, are listed in Table 2 and are plotted in Fig. 8. Figure 8 also gives the values measured by Littauer and Walker at  $135^\circ$  for beryllium and carbon and those obtained by Peterson, Gilbert, and White at  $45^\circ$ ,  $90^\circ$ , and  $135^\circ$  for carbon. Table 2 also gives the relative yield per proton and per neutron of the mesons from beryllium and carbon.

The lack of variation with angle of the ratio agrees well with the angular variation predicted assuming a magnetic interaction between the photon and nucleon. It is not possible, however, with the statistics

that were obtained to judge the validity of using the values of the static nucleon moments.

The curves obtained by Brueckner were for free nucleons and the absolute values of the beryllium ratios do not agree with the values predicted in that case, although the ratio for carbon, where there are an equal number of neutrons and protons, is not greatly different.

If we assume that the beryllium nucleus acts as a group of four protons and four neutrons closely bound, plus an almost free neutron, and further assume that the minus to plus ratio from the eight closely bound nucleons is the same as that for the twelve nucleons in carbon, the production of negative mesons from the almost free neutron can be found relative to one of the bound neutrons in beryllium. In this way, using the values of the minus to plus ratios for beryllium and carbon at  $90^\circ$  as measured in this experiment, a value of  $2.2 \pm 0.4$  for the ratio of production from loosely and tightly bound neutrons in beryllium is obtained. The value found by Mozley<sup>16</sup> for the production ratio between a free proton and one bound in beryllium was  $2.3 \pm 0.4$ . The agreement between this number and that for the negative meson ratio as determined above is probably largely fortuitous, but it suggests one way in which the large value of the beryllium ratio might be produced.

TABLE 2

Angle	Beryllium	Carbon
60°	1.93 ± 0.12	
90°	1.96 ± 0.10	1.27 ± 0.06
150°	1.92 ± 0.11	

Ratio of beryllium to carbon positive meson yield per proton

1.24 ± 0.09 (90°)

Ratio of beryllium to carbon negative meson yield per neutron

1.44 ± 0.08 (90°)

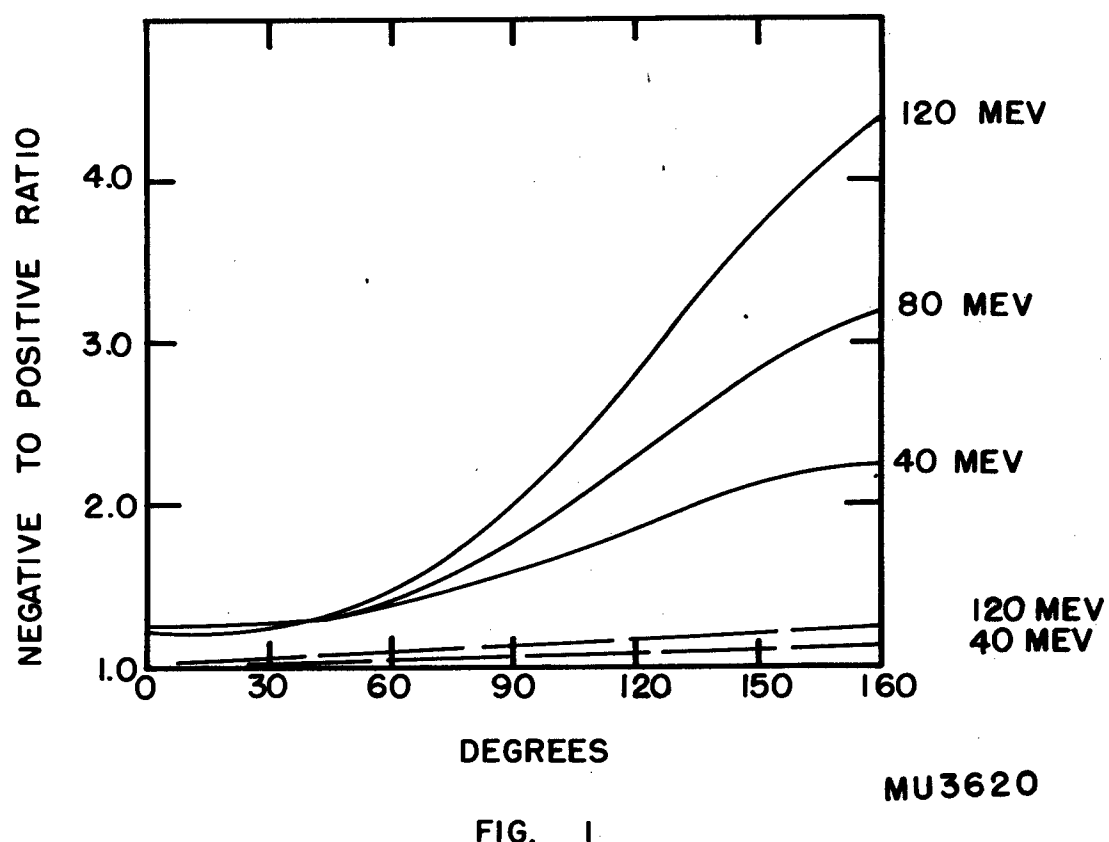
The limits shown are in terms of standard deviation.

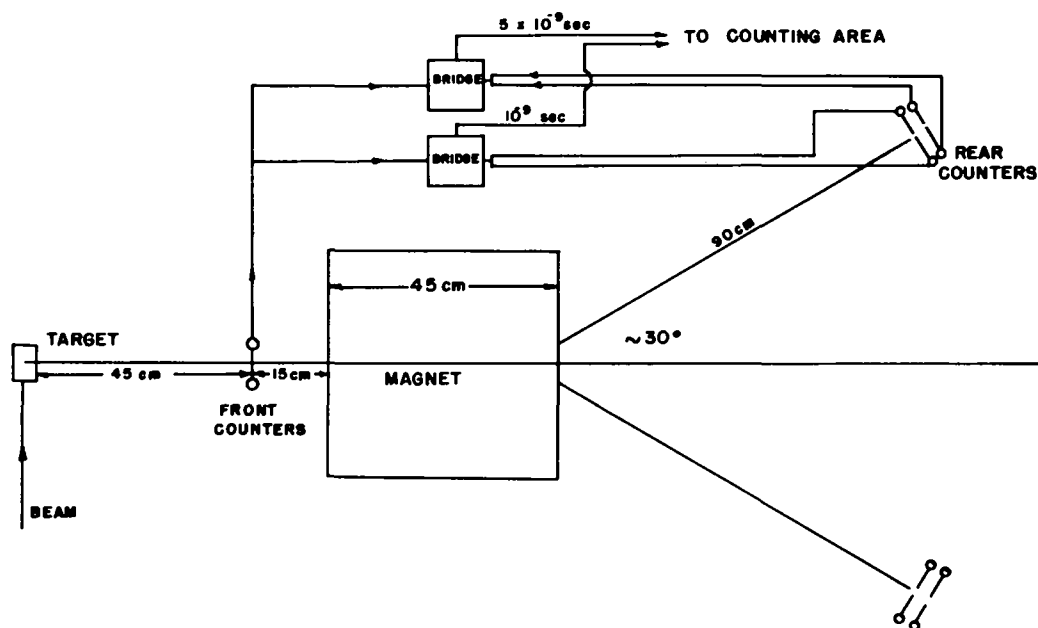
IV ACKNOWLEDGMENTS

I wish to thank Professor E. M. McMillan for his support and helpful advice in this experiment. My sincere gratitude goes to Dr. W. K. H. Panofsky who suggested the experiment and who was always available for consultation and help. Thanks are also due to Mr. Leland Neher, who assisted materially in the development of the identification scheme used and who offered valuable advice in all parts of the experiment, and to Mr. Calvin André, who spent many after midnight hours helping to set up and take down the equipment. The members of the synchrotron crew, under George McFarland were invariably cooperative and helpful. I would like to thank in particular Rudin Johnson, Al Waugh, and Ken Crebbin for their help with the equipment at different times.

V REFERENCES

1. E. M. McMillan, J. Peterson, and R. S. White, *Science* 110, 579 (1949)
2. J. Peterson, W. Gilbert, and R. S. White, *Physical Review* 81, 1003 (1950)
3. K. Brueckner and M. Goldberger, *Physical Review*, 76, 1725 (1945)
4. K. A. Brueckner, *Physical Review*, 79, 641 (1950)
5. R. S. White, PhD Thesis, University of California 1951
6. J. Steinberger and A. S. Bishop, *Physical Review*, 78, 493 (1950)
7. M. Jakobson, A. Schulz, and J. Steinberger, *Physical Review*, 81, 894 (1951)
8. R. M. Littauer and D. Walker, *Bulletin of the American Physical Society*, 26, #3 F3; *Physical Review*, 82, 746 (1951)
9. R. F. Post and N. S. Shiren, *Physical Review* 78, 80 (1950)
10. I. L. Lebow, B. T. Feld, D. H. Frisch, and L. S. Osborne, *Physical Review*, 85, 681 (1952)
11. H. A. Medicus, *Physical Review* 83, 662 (1951)
12. M. Camac, et al., *Physical Review*, 82, 745 (1951)
13. M. Jakobson, PhD Thesis, University of California 1951
14. D. Stork, *Private communication*
15. C. Chedester, P. Isaacs, A. Sachs, and J. Steinberger, *Physical Review*, 82, 958 (1951)
16. R. F. Mozley, UCRL-706 (Revised)

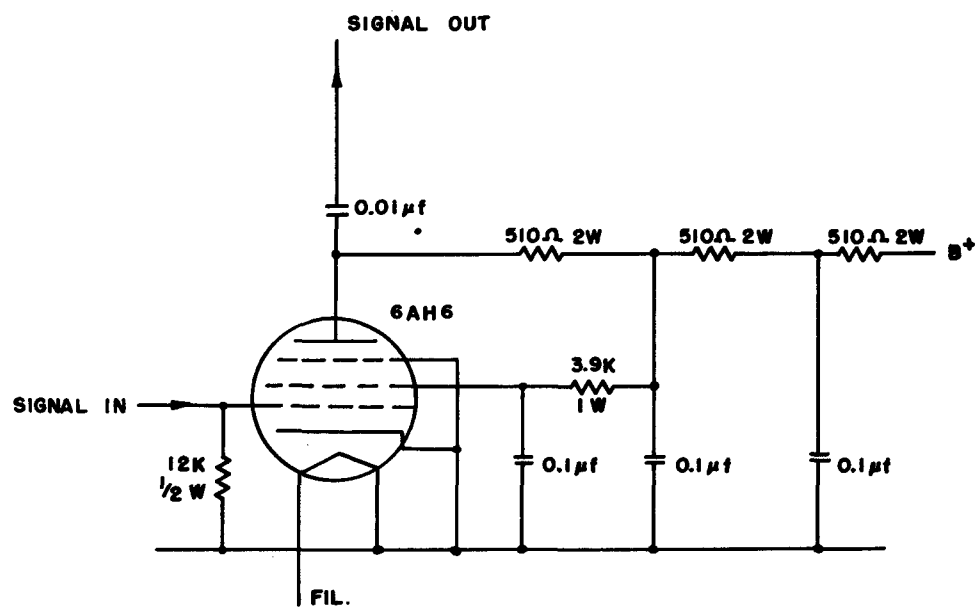




PHYSICAL ARRANGEMENT OF THE APPARATUS

FIG. 2

MU3621



PULSE LIMITER

MU3 622

FIG. 3

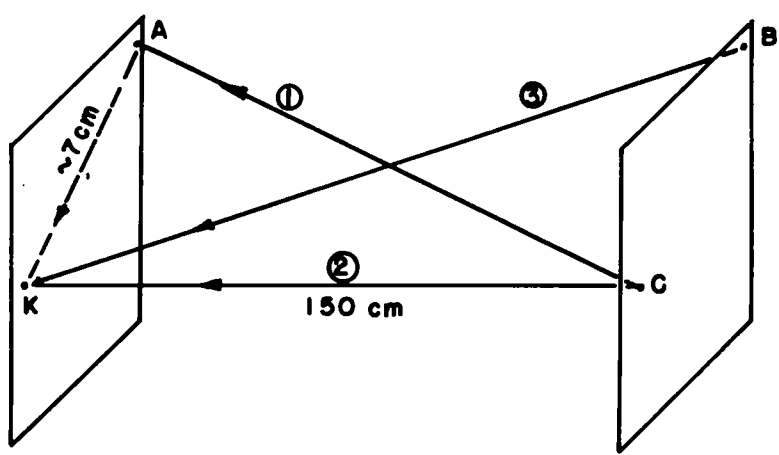


FIG. 4

**MU3623**

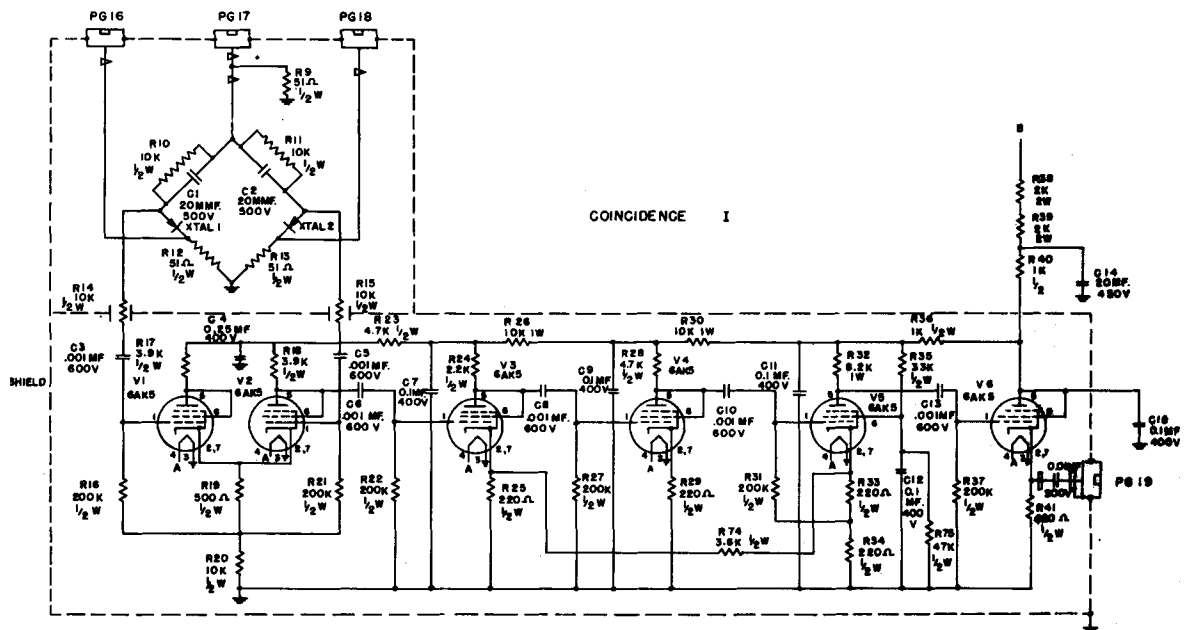


FIG. 5

MU3624

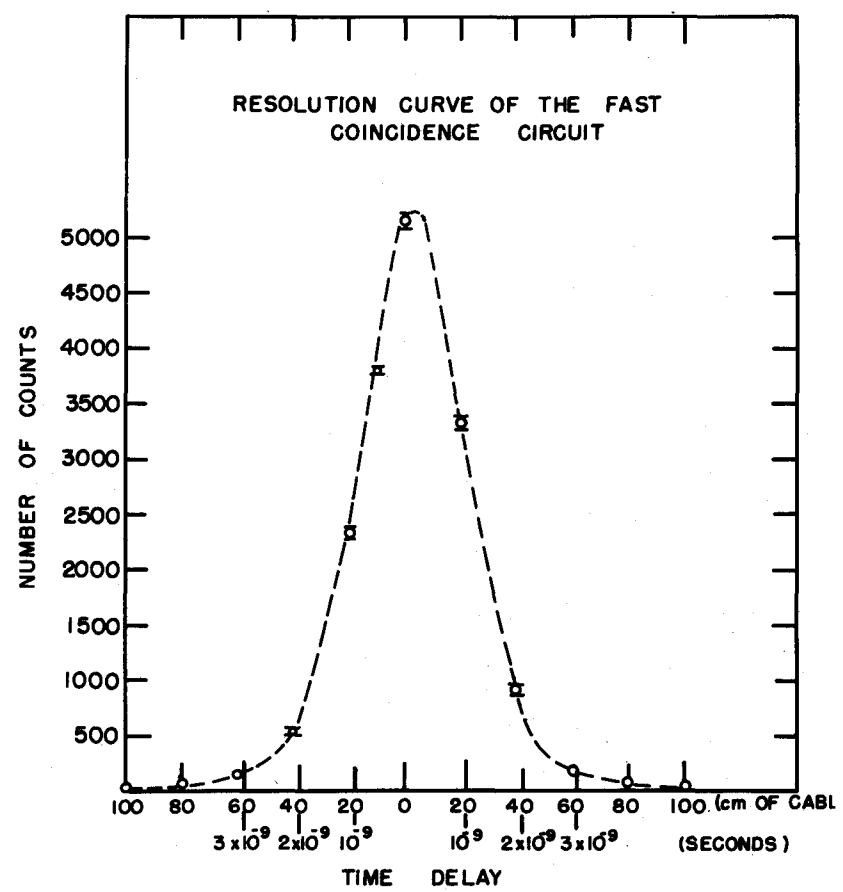
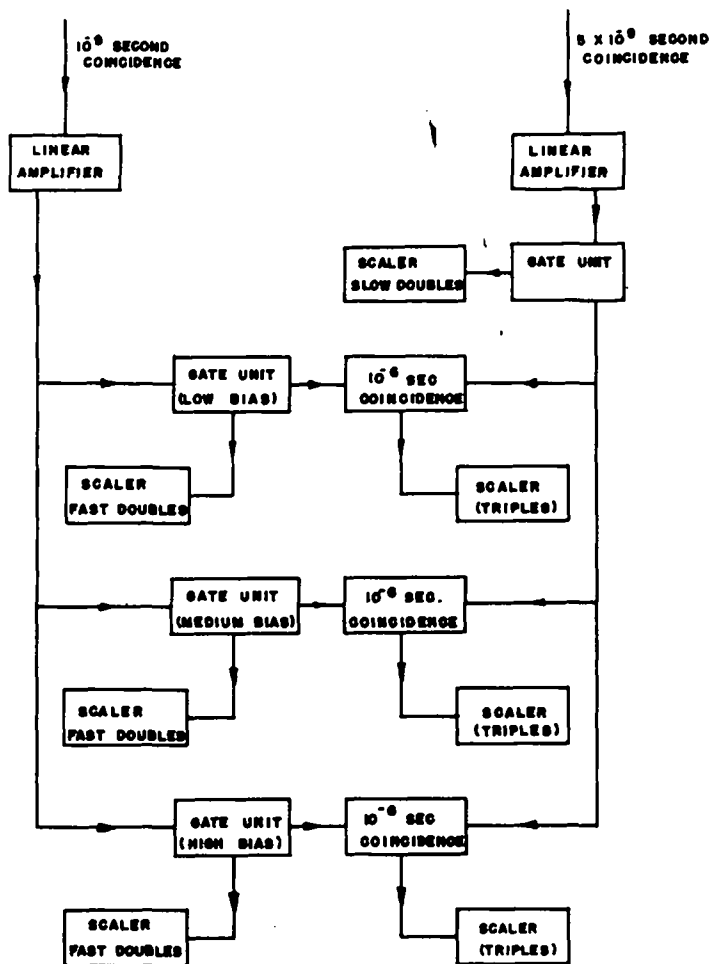


FIG. 6

MU3625



BLOCK DIAGRAM OF COUNTING AREA ELECTRONICS

FIG. 7

MU3626

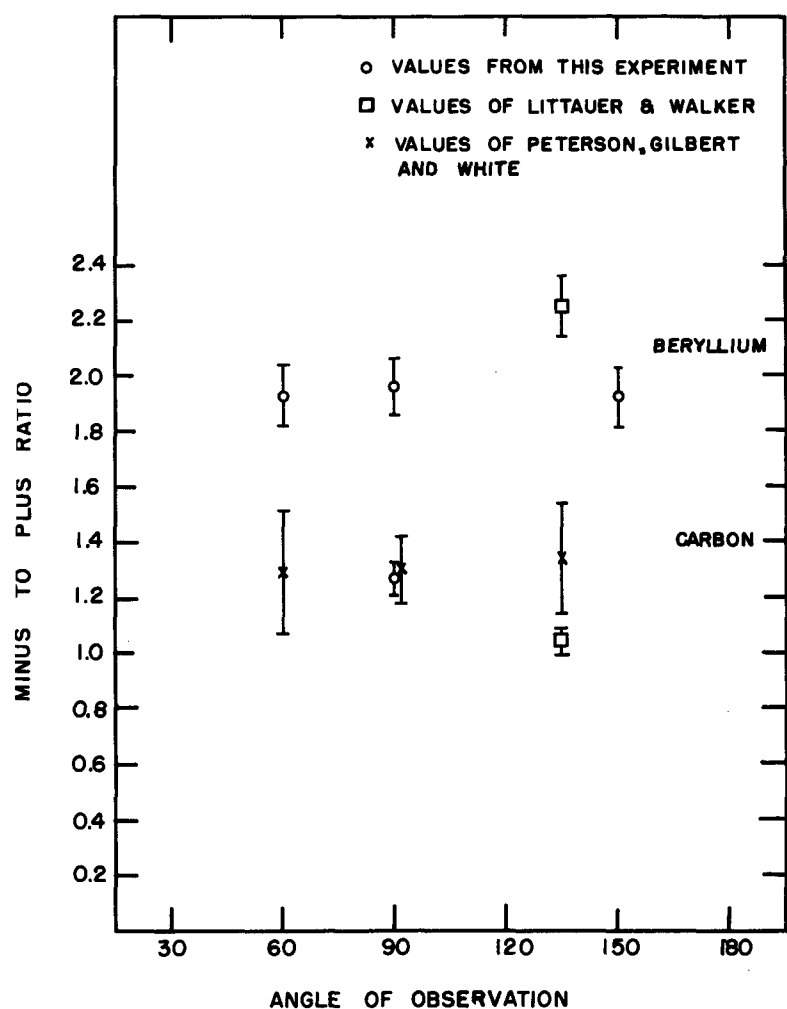


FIG. 8

MU3627